Laser illuminated imaging: multiframe beam tilt tracking and deconvolution algorithm

Capt. David J. Becker
Air Force Institute of Technology
Dr. Stephen C. Cain
Air Force Institute of Technology

1. ABSTRACT

A laser-illuminating imaging system operating in the presence of atmospheric turbulence will encounter several sources of noise and diffraction induced errors that can make postprocessing the images difficult. As the beam propagates, turbulence induced tilt will cause the beam to wander off axis from the target. This is especially troublesome in imaging satellites due to most turbulence being closer to the Earth's surface and greatly affecting the beam in the early stages of propagation. Additionally, the returning beam convoluted with the target will encounter turbulence induced tilt that appears as apparent movement of the target between image frames. This results in varying beam intensities at the target surface between imaging frames that can affect registration algorithms. Using simulated data, an algorithm using expectation maximization and least squares techniques was developed that has the ability to estimate both the tilt of the pulsed laser beam and the apparent movement of the object between incoherent frames separately and produce a superior estimate of the target. The results from this algorithm can be used to reduce the effects of beam wander and thus increase the SNR of postprocessed images.

2. INTRODUCTION

When high resolution imagery is desired from laser radar (LADAR) imaging systems there are several factors that can limit the systems performance such as diffraction from the LADAR optics, atmospheric turbulence and laser beam speckle. These factors can severely distort the image quality and reduce the resolution of the measured data in each frame as shown in Fig. 1. Due to operating conditions and factors such as cost, size and weight, an adaptive optics approach may not be feasible for all situations. This is where the benefits of a postprocessing algorithm can be exploited to improve the quality of LADAR imagery. The algorithms studied in this report can provide near real time estimates of the target image with the distortions such as speckle, blurring and defocus significantly reduced when multiple frames of data are available.

In a LADAR application, diffraction due to the atmospheric turbulence results in primarily tilt, blur and defocus which account for over 93% of phase error [1]. Atmospheric turbulence causes random time delays in light as it propagates through the atmosphere, using Fourier optics this time delay or tilt in the propagation field can be represented as a spatial shift in the image field [2]. Each pulse of the laser beam is randomly shifted to a different position on the target and the returning field after propagation is again shifted and blurred. Additionally, in a LADAR system, speckle is a significant source of noise. Speckle is caused by the coherency of the illuminating laser source, combined with the rough surface of the target [3]. Each frame of data will contain independent intensity fluctuations that appear as bright and dark spots as a result of laser speckle.

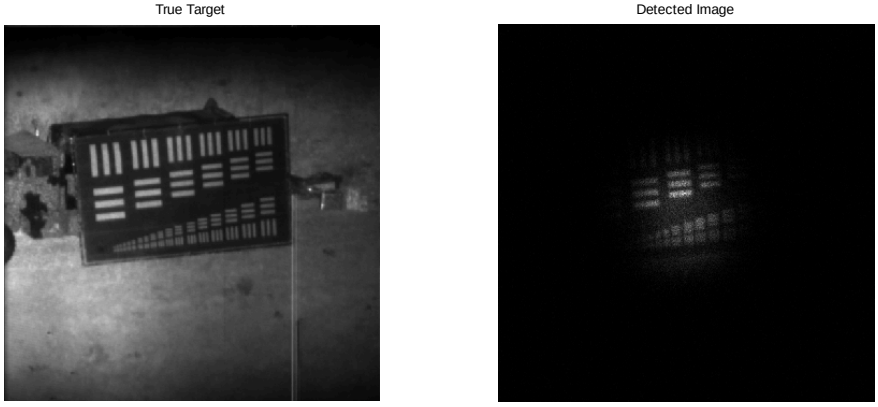

Fig. 1 Example of true target and beam limited detected image with diffraction and speckle

Report Documentation Page

Form Approved
OMB No. 0704-0188

1. REPORT DATE	2. REPORT TYPE	3. DATES COVERED
SEP 2012		**00-00-2012 to 00-00-2012**

4. TITLE AND SUBTITLE	5a. CONTRACT NUMBER
Laser illuminated imaging: multiframe beam tilt tracking and deconvolution algorithm	5b. GRANT NUMBER
	5c. PROGRAM ELEMENT NUMBER
6. AUTHOR(S)	5d. PROJECT NUMBER
	5e. TASK NUMBER
	5f. WORK UNIT NUMBER
7. PERFORMING ORGANIZATION NAME(S) AND ADDRESS(ES) **Air Force Institute of Technology,Wright Patterson AFB,OH,45433**	8. PERFORMING ORGANIZATION REPORT NUMBER
9. SPONSORING/MONITORING AGENCY NAME(S) AND ADDRESS(ES)	10. SPONSOR/MONITOR'S ACRONYM(S)
	11. SPONSOR/MONITOR'S REPORT NUMBER(S)

12. DISTRIBUTION/AVAILABILITY STATEMENT
Approved for public release; distribution unlimited

13. SUPPLEMENTARY NOTES
In Advanced Maui Optical and Space Surveillance Technologies Conference (AMOS), 11-14 Sep 2012, Maui, HI.

14. ABSTRACT
A laser-illuminating imaging system operating in the presence of atmospheric turbulence will encounter several sources of noise and diffraction induced errors that can make postprocessing the images difficult. As the beam propagates, turbulence induced tilt will cause the beam to wander off axis from the target. This is especially troublesome in imaging satellites due to most turbulence being closer to the Earth?s surface and greatly affecting the beam in the early stages of propagation. Additionally, the returning beam convoluted with the target will encounter turbulence induced tilt that appears as apparent movement of the target between image frames. This results in varying beam intensities at the target surface between imaging frames that can affect registration algorithms. Using simulated data, an algorithm using expectation maximization and least squares techniques was developed that has the ability to estimate both the tilt of the pulsed laser beam and the apparent movement of the object between incoherent frames separately and produce a superior estimate of the target. The results from this algorithm can be used to reduce the effects of beam wander and thus increase the SNR of postprocessed images.

15. SUBJECT TERMS

16. SECURITY CLASSIFICATION OF:			17. LIMITATION OF ABSTRACT	18. NUMBER OF PAGES	19a. NAME OF RESPONSIBLE PERSON
a. REPORT **unclassified**	b. ABSTRACT **unclassified**	c. THIS PAGE **unclassified**	**Same as Report (SAR)**	**8**	

3. PREVIOUS WORK

Previously, a blind deconvolution algorithm has been developed to improve the quality of imagery affected by the atmosphere's optical transfer function (OTF) and laser speckle by time averaging multiple deconvolved and registered frames [4]. This algorithm uses the Ayers-Dainty blind deconvolution technique [5], however its algorithm doesn't take into account the beam shifting off axis between each frame of data. Another technique commonly used in blind deconvolution problems is the expectation maximization (EM) algorithm developed by Dempster, Laird and Rubin [6]. The EM algorithm is an iterative approach to computing the maximum likelihood estimate of the unknown variables. A benefit when working with EM algorithms is that their convergence is assured since the algorithm is guaranteed to increase the likelihood function at each iteration.

This paper uses the EM algorithm approach to develop a set of equations that can iteratively solve for the complete data by solving for the target or complete data, the global shifts and the beam shifts separately in each frame.

4. SYSTEM ANALYSIS

The imaging system simulated in this report represents a LADAR system that uses a coherent laser source. The target is illuminated by the laser beam and the returning field is distorted by atmospheric turbulence causing tilting, blurring and other higher order [4] effects on the returned image. Additionally the intensity of the field will contain random speckle fluctuations. The returned image is limited by the size of the beam and thus beam wander results in each frame being illuminated at a different position and with a different intensity than the previous frame.

An expression for the image obtained from the system is shown in Eq. 1 where i_k is the k^{th} measured data frame which is the true image, o, multiplied by the beam, b, and convoluted with h, the atmospheric point spread function (PSF). The global shifts are represented in the PSF as α_k and β_k and the beam shifts are represented as γ_k and ε_k.

$$i_k = \sum_z \sum_w o(z,w) b(z-\gamma_k, w-\varepsilon_k) h(x-z-\alpha_k, y-w-\beta_k) \quad (1)$$

4.1 Atmospheric Turbulence

Turbulence in Earth's atmosphere is caused by random variations in temperature and air motion which changes the refractive index of the air [7]**.** As optical waves propagate in Earth's atmosphere, the wave is distorted by the changes in the refractive index of the air it is traveling through. The variance in the phase of the field [1] as a result of the turbulence is described by Eq. 2 where D is the diameter of the receiver aperture and r_0 is the coherence diameter. The coherence diameter or seeing parameter is typically used to describe the optical quality of the atmosphere and is typically around 5-10 cm for averaging viewing sites and up to 20 cm for the best viewing sites.

$$\sigma^2 = 1.03\left(\frac{D}{r_0}\right)^{5/3} \quad (2)$$

The phase variance due to tilt [1] in one axis is given by Eq. 3, this variance is doubled when looking at both axis. Nearly 87% of the total phase variance is a result of tilt with image distorting effects such as blurring and defocus making up the rest. Tilt can be successfully removed by an image registration algorithm. However, the higher order image distortions with a residual phase variance given in Eq. 4 are compensated for using a blind deconvolution algorithm.

$$\sigma_\alpha{}^2 = 0.448\left(\frac{D}{r_0}\right)^{5/3} \quad (3)$$

$$\sigma^2{}_{tilt\ removed} = 0.134\left(\frac{D}{r_0}\right)^{5/3} \quad (4)$$

4.2 Noise

The majority of noise in a LADAR system can be attributed to one of the following sources: photon counting noise, laser speckle and background noise. Laser speckle is the result of imaging a surface, rough on the scale of an optical

wavelength, using the coherent light from a laser [8]. The rough surface of an object cause incoming light to reflect off at random different angles resulting in a multitude of amplitude spread functions produced from each point on the target interfering with one another at the detector. The variance of the laser speckle, shown in Eq. 5, has a negative binomial distribution [8] and is dependent of the coherency of the light and the expected number of photons received. An example of this phenomenon is shown in Fig. 2b, the image has a random intensity modulation that severely distorts the image quality when compared to the image obtained from an incoherent light source shown in Fig. 2a.

$$\sigma_{speckle}^2 = E[N_{signal}]\left(1 + \frac{E[N_{signal}]}{M}\right) \quad 5$$

Where,

- $E[N_{signal}]$is the expected number of photons
- $M$is the coherency parameter of the light, 1 = fully coherent, □ = fully incoherent

(a) (b)

Fig. 1 Incoherent imaging and coherent imaging with only speckle noise

Speckle noise can be reduced by using a time average of properly registered images. Depending on the coherence of the light, the speckle pattern introduced to each image can be especially troublesome when registering the images. If image quality is poor, the algorithm might not properly register each image frame and will blur the image. However, a blind deconvolution algorithm used to remove the effects of the atmosphere should be able to improve the quality because the blurring effect from improperly registered frames is similar to the blurring effect from the atmosphere.

Photon counting noise occurs due to the randomness of counting photo-electrons at the detector and follows a Poisson distribution. Additionally background noise is the result of radiation sources besides the illuminating beam that are counted by the detector. The amount of background noise can be measured by taking images with the illuminating laser not on.

5. METHOD

The proposed approach to reduce the effects of the atmospheric turbulence and speckle pattern of imagery obtained from a LADAR system is to develop an EM algorithm that accounts for the global shift and the beam shift in each frame. This paper describes the mathematics in developing this algorithm and then the implementation issues with the mathematical solution. Going into the derivation it is assumed that the beam shape is known and can be described with a Gaussian intensity profile. Additionally the shape of the PSF is known, however the tilt or shifts are not and also the background radiation can be measured. These assumptions are not unrealistic for many LADAR applications.

5.1 Multiframe Postprocessing Algorithm

Similar to many deconvolution algorithms, the expectation maximization blind deconvolution algorithm is modeled after Poisson statistics due to the ease of working with Poisson statistics. Following the steps outline by Dempster, Liard and Rubin [6], first, a statistical model for the incomplete data is defined in Eq. 6. It is known that the incomplete data, *d*, is an image array of independent Poisson random variables multiplied by the beam with

unknown shifts and convoluted with the shifted PSF. The measured background radiation is represented as B in the equation.

$$E[d(x,y)] = \sum_k \sum_z \sum_w o(z,w)b(z-\gamma_k, w-\varepsilon_k)h(x-z-\alpha_k, y-w-\beta_k) + B \tag{6}$$

The complete or desired data is related to the incomplete data through the relationship shown below in Eq. 7.

$$d_k(x,y) = \sum_z \sum_w \widetilde{d_k}(x,y,z,w) + \widetilde{d_B} \tag{7}$$

The complete data is also considered to be Poisson so that a statistical model of the incomplete data can be related to the complete data through Eq. 8 and 9. Choosing the complete data to be Poisson is acceptable because the sum of Poisson random variables is also a Poisson random variable [3].

$$E\left[\widetilde{d_k}(x,y,z,w)\right] = o(z,w)b(z-\gamma_k, w-\varepsilon_k)h(x-z-\alpha_k, y-w-\beta_k) \tag{8}$$

$$E\left[\widetilde{d_B}\right] = B \tag{9}$$

The algorithm is derived from the probability mass function (PMF) for a Poisson process [3] given in Eq. 10 where k is the number of occurrences and λ is the rate of those occurrences.

$$P[k] = \frac{\lambda^k e^{-\lambda}}{k!} \tag{10}$$

Using Eq. 10 and applying the model for the complete data in Eq. 8, results in the complete data likelihood expression:

$$P\left[\widetilde{d_k}(x,y,z,w)\right] = \frac{o(z,w)b(z-\gamma_k, w-\varepsilon_k)h(x-z-\alpha_k, y-w-\beta_k)^{\widetilde{d_k}(x,y,z,w)} e^{-o(z,w)b(z-\gamma_k, w-\varepsilon_k)h(x-z-\alpha_k, y-w-\beta_k)^{\widetilde{d_k}(x,y,z,w)}}}{\widetilde{d_k}(x,y,z,w)!} \tag{11}$$

Expanding Eq. 11 by solving for all pixel points in the image array results in Eq. 12:

$$P\left[\widetilde{d_k}(x,y,z,w)\ \forall\ x,y,z,w\right] = \prod_k \prod_x \prod_y \prod_z \prod_w \frac{o(z,w)b(z-\gamma_k, w-\varepsilon_k)h(x-z-\alpha_k, y-w-\beta_k)^{\widetilde{d_k}(x,y,z,w)} e^{-o(z,w)b(z-\gamma_k, w-\varepsilon_k)h(x-z-\alpha_k, y-w-\beta_k)^{\widetilde{d_k}(x,y,z,w)}}}{\widetilde{d_k}(x,y,z,w)!} \tag{12}$$

Following the EM steps, the natural log is taken to get the log-likelihood in Eq. 13. Greatly simplifying this expression is that the products are turned into summations when the natural log is taken.

$$\begin{aligned} L(o,\alpha_k,\beta_k,\gamma_k,\varepsilon_k) = \sum_k \sum_x \sum_y \sum_z \sum_w \widetilde{d_k}(x,y,z,w) \ln\big(o(z,w)b(z-\gamma_k, w-\varepsilon_k)h(x-z-\alpha_k, y-w-\beta_k)\big) \\ - o(z,w)b(z-\gamma_k, w-\varepsilon_k)h(x-z-\alpha_k, y-w-\beta_k) - \ln\left(\widetilde{d_k}(x,y,z,w)\right)! \end{aligned} \tag{13}$$

The expectation step of the EM algorithm takes the conditional expectation of the complete data log likelihood when given the incomplete data and past estimates of the unknown parameters. This derivation is extensive, however the resulting expression is given below:

$$\begin{aligned} E\left[\left(L(o,\alpha_k,\beta_k,\gamma_k,\varepsilon_k)\middle| o^{old}, d_k(x,y), \alpha_k^{old}, \beta_k^{old}, \gamma_k^{old}, \varepsilon_k^{old}\right)\right] \\ = \sum_k \sum_x \sum_y \sum_z \sum_w \frac{o^{old}(z,w)b\left(z-\gamma_k^{old}, w-\varepsilon_k^{old}\right)h\left(x-z-\alpha_k^{old}, y-w-\beta_k^{old}\right)d(x,y)}{{i_k}^{old}(x,y)} \ln\big(o(z,w)b(z-\gamma_k, w \\ -\varepsilon_k)h(x-z-\alpha_k, y-w-\beta_k)\big) - o(z,w)b(z-\gamma_k, w-\varepsilon_k)h(x-z-\alpha_k, y-w-\beta_k) \end{aligned} \tag{14}$$

Where,

$$i_k{}^{old} = \sum_z \sum_w o^{old}(z,w) b\left(z - \gamma_k^{old}, w - \varepsilon_k^{old}\right) h\left(x - z - \alpha_k^{old}, y - w - \beta_k^{old}\right)$$

The maximization step of the EM algorithm maximizes the conditional expected value of the complete data log-likelihood from Eq. 14 with respect to the parameters being estimated for a single frame, k_0. This process is completed for the three different set of unknowns: the global shifts, the beam shifts, and the true object. In each instance, the terms not dependent on the parameters being estimated can be dropped. Again, due to extensive calculations required to prove each likelihood expression, the results for each of the three unknown parameter sets are given below.

$$L_{\alpha,\beta} = \sum_z \sum_w o^{old}(z,w) b\left(z - \gamma_{k_0}^{old}, w - \varepsilon_{k_0}^{old}\right) \sum_x \sum_y \frac{d_{k_0}(x,y)}{i^{old}(x,y)} h\left(x - z - \alpha_{k_0}^{old}, y - w - \beta_{k_0}^{old}\right) \ln\left(h\left(x - z - \alpha_{k_0}, y - w - \beta_{k_0}\right)\right) \quad (15)$$

$$L_{\gamma,\varepsilon} = \sum_z \sum_w o^{old}(z,w) b\left(z - \gamma_{k_0}^{old}, w - \varepsilon_{k_0}^{old}\right) \ln\left(b\left(z - \gamma_{k_0}, w - \varepsilon_{k_0}\right)\right) \sum_x \sum_y \frac{d_{k_0}(x,y)}{i_{k_0}{}^{old}(x,y)} h\left(x - z - \alpha_{k_0}^{old}, y - w - \beta_{k_0}^{old}\right) - \sum_z \sum_w o(z,w) b\left(z - \gamma_{k_0}, w - \varepsilon_{k_0}\right) \quad (16)$$

$$\hat{o}(z_0, w_0) = \frac{\sum_k o^{old}(z_0, w_0) b\left(z_0 - \gamma_k^{old}, w_0 - \varepsilon_k^{old}\right) \sum_x \sum_y \frac{d_k(x,y)}{i_k{}^{old}(x,y)} h\left(x - z_0 - \alpha_k^{old}, y - w_0 - \beta_k^{old}\right)}{\sum_k b(z_0 - \gamma_k, w_0 - \varepsilon_k)} \quad (17)$$

These derived equations show that a mathematical solution to solving for each of the parameters individually is possible by an iterative process that first estimates the object, $\hat{o}$, then estimates the global shift parameters, α and β, then estimates the beam shifts, γ and ε. This EM algorithm is guaranteed to converge to the correct solution. However a problem exists in the implementation of the two likelihood expressions describing the shifts. In both instances, MATLAB was unable to evaluate the natural log of the shifting beams or PSFs with enough accuracy to correctly estimate the shift. The non-linear properties of the natural log function caused the changes between the beam shifts or the PSF shifts from each frame to be smaller than its precision. This derivation does however prove that a more accurate estimate of the object can be found if the beam shifts can be estimated.

5.2 Least Squares Likelihood

An iterative least squares likelihood approach was taken to solve for the global and beam shifts. Each iteration moves the estimate closer to the solution. This technique is accomplished one frame at a time for first the global shifts and then for the beam shifts. Fig. 2 shows the flow of this technique for estimating the beam shifts, estimating the PSF shifts is exactly the same so it is not shown here.

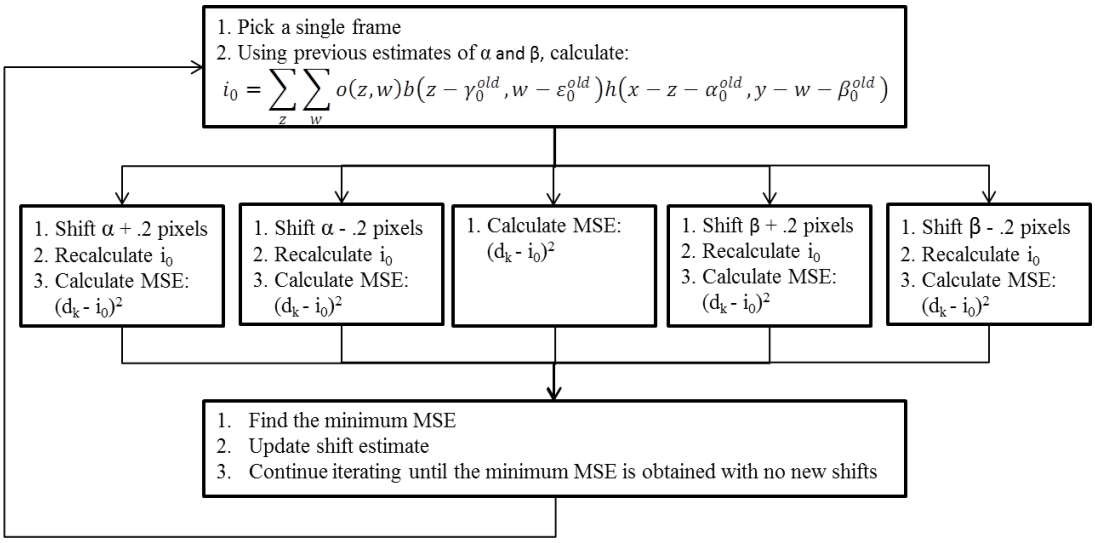

Fig. 2 Iterative least squared error algorithm

6. SIMULATION & RESULTS

A combination of the object estimation using the EM algorithm in Eq. 17 and the shift estimation using the least squares algorithm was developed in MATLAB using the system characteristics in Table 1. The algorithm was tested using simulated data. All shifts were random uncorrelated Gaussian variables, the beam shifts had a standard deviation of 9 pixels and the global shifts had a standard deviation of 3 pixels.

Each frame of the simulated data was created by shifting the unit amplitude Gaussian beam by its random shift and multiplied by the target frame and then convoluted with a non-shifted PSF. Fourier optics properties were used to propagate the source to the image plane. The image detected was then shifted to simulate the tilt component of the PSF. Speckle was added to each frame by applying a negative binomial random variable to each pixel point in the imaging plane. All convolutions were done by transforming into the Fourier domain and multiplying.

Table 1 Simulation parameters

Receiver aperture diameter, D	.3 m
Beam width, w_0	.08 m
Wavelength	1.55 μm
Propagation distance	10 km
Coherence factor, M	40
Number of frames	30
Max number of photons in return pulse	100 photons
Background light	1 photon
Number of iterations	20
Pixel shift resolution	.2 pixels

The root mean squared error (RMSE) was calculated at each iteration since simulated data used and the truth image was known using Eq. 18, where $\hat{o}$ is the estimated image produced at that iteration and o is the known true image.

$$RMSE = \frac{\sum_{x=1}^{N}\sum_{y=1}^{N}(\hat{o}(x,y) - o(x,y))}{N^2} \quad 18$$

The RMSE was first calculated using the algorithm developed and then calculated again using the same algorithm except the beam shifts were not estimated. The results, in Fig. 3 and Table 2, show that when the beam position was estimated, the algorithm did a better job at estimating the object. The estimated image at the iteration with the minimum error is shown in Fig. 4.

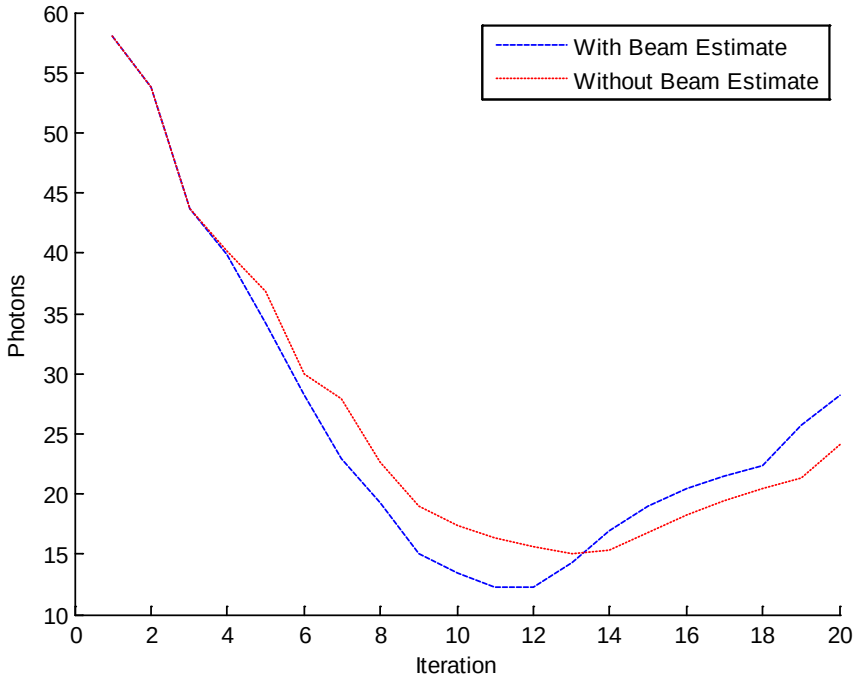

Fig. 3 Algorithm RMSE at each iteration

Table 2 Minimum photon error with and without beam estimation

	# of iterations	Min RMSE
With beam estimate	11	12.26 photons
Without beam estimate	13	15.01 photons

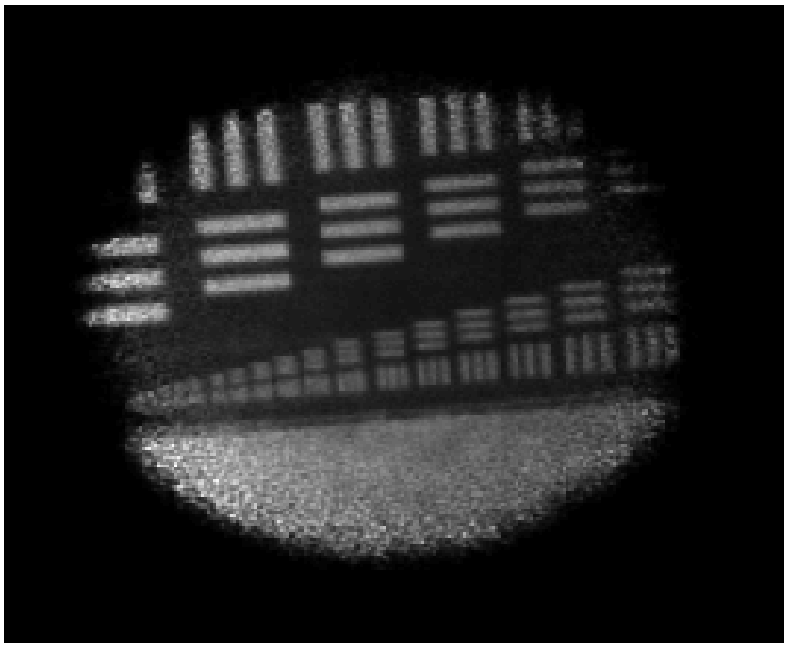
Fig. 4 Estimated object at iteration 11

Since simulated data was used, the actual beam and global shifts were compared to their estimated values. The mean of the minimum error difference is shown in Table 3. Interestingly, the difference between the actual and estimated shift values is not minimized at the same iteration as the object but several iterations afterwards. This seems to imply that the shift estimators performance improves as the object estimate improves.

Table 3 Error in shift estimation

	Mean Difference Error
α	.5939 pixels
β	.4137 pixels
γ	1.2586 pixels
ε	.7887 pixels

7. FUTURE WORKS

There are several processes in this algorithm that need to be further studied. First, the EM algorithm originally developed would be the ideal solution since it is guaranteed to converge and can't fall into a local minimum value like the least squares approach. This might produce shift estimation results that are more accurate and likely further increase the performance of the algorithm. Additionally, the iterative approach needs defined stopping criteria when working with non-simulated data. This might include iterating the beam and global shifts until a minimum error is estimated and then going back and again estimating the object with these better shift parameters. Lastly, noise in this simulation was limited to speckle and background noise and a more accurate model should be used to get a more accurate performance baseline.

8. CONCLUSION

When imaging with a LADAR system, image quality is severely reduced due to atmospheric turbulence and laser speckle noise. Previous algorithms have been able to compensate for these degradations using blind deconvolution and image registration techniques. However, these algorithms do not take into account the movement of the beam between frames due to atmospheric induced tilt. The algorithm developed in this paper estimated the beam shifts along with the global shifting between frames to produce an estimate of the object with significantly less effects from atmospheric turbulence and speckle noise. Additionally, it was able to estimate the beam and global shifts while producing an estimated image that had less error than an estimate of the object when the beam was not tracked.

9. REFERENCES

1. Robert J. Noll, "Zernike polynomials and atmospheric turbulence," J. Opt. Soc. Am. 66, 207-211 (1976)
2. Goodman, Joseph W., *Introduction to Fourier Optics*, Greenwood Village, CO: Roberts & Company Publishers, 2005. 0-9747077-2-4.
3. Goodman, Joseph W., *Statistical Optics*, Wiley, New York : John Wiley & Sons Inc, 1985. 0-471-01502-4
4. Dayton, D., Browne, S., Gonglewski, J., Sandven, S., Gallegos, J. and Shilko, M., "Long-range laser illuminated imaging: analysis and experimental demonstrations," Soc. of Photo-Optical Instrumentation Engineers, 1001-1009 (June 2001)
5. Ayers, G. R. and Dainty, J. C., "Iterative blind deconvolution method and its applications," Opt. Lett. 13, 547-549 (1988)
6. Dempster, A. P., Laird, N. M. and Rubin, D. B., "Maximum likelihood from in-complete data via the em algorithm," Journal of the Royal Statistical Society: Series B, 39(1):1–38, November 1977.
7. Andrews, Larry C., Phillips, Ronald L., *Laser Beam Propagation through Random Media*, 2nd Ed. Bellingham, Washington: SPIE Press, 2005.
8. Richmond, Richard D., Cain, Stephen C., *Direct-Detection LADAR Systems*, 1st Ed. Bellingham, Washington: SPIE Press, 2010. 978-0-8194-8072-9.